

Contents lists available at ScienceDirect

## Palaeogeography, Palaeoclimatology, Palaeoecology

journal homepage: www.elsevier.com/locate/palaeo





# Proxies for paleo-oxygenation: A downcore comparison between benthic foraminiferal surface porosity and I/Ca

Wanyi Lu<sup>a,\*</sup>, Catia F. Barbosa<sup>b</sup>, Anthony E. Rathburn<sup>c</sup>, Priscila da Matta Xavier<sup>b</sup>, Anna P. S. Cruz<sup>b,c</sup>, Ellen Thomas<sup>d,e</sup>, Rosalind E.M. Rickaby<sup>f</sup>, Yi Ge Zhang<sup>g</sup>, Zunli Lu<sup>a</sup>

- <sup>a</sup> Department of Earth & Environmental Sciences, Syracuse University, Syracuse, NY, USA
- <sup>b</sup> Programa de Pós Graduação em Geoquímica, Universidade Federal Fluminense, Niterói, RJ, Brazil
- Department of Geological Sciences, California State University, Bakersfield, CA, USA
- <sup>d</sup> Department of Earth and Planetary Sciences, Yale University, New Haven, CT, USA
- <sup>e</sup> Department of Earth and Environmental Sciences, Wesleyan University, Middletown, CT, USA
- f Department of Earth Sciences, University of Oxford, Oxford, UK
- g Department of Oceanography, Texas A&M University, College Station, TX, USA

## ARTICLE INFO

Editor: A Dickson

Keywords: Bottom water Oxygen Benthic foraminifera Iodine Surface pores

#### ABSTRACT

Benthic foraminiferal surface porosity (the mean percentage of surface area covered by pores; higher porosity: lower oxygenation) and iodine to calcium ratio (I/Ca, higher I/Ca: higher oxygenation) are both promising paleoceanographic proxies that will advance through testing in down-core studies. Here we report the first down-core comparison (~45 kyr) of these proxies for a core from the southern Brazilian margin (26°40.22′ S, 46°26.46′ W, 475 m water depth). Both proxies are most sensitive to low-O2 conditions (<50  $\mu$ mol/kg, and not well-constrained at higher O2 concentrations. Porosity values are generally low (<15%) and I/Ca ranges between ~4 and ~6  $\mu$ mol/mol throughout the core. The two proxies are overall consistent, suggesting that bottom-water oxygen concentrations at the site remained above 50  $\mu$ mol/kg during the last 45 kyr. Several non-O2 factors (e.g., iodate reduction rates, water mass mixing, temperature, foraminiferal shell robustness) could influence the proxies and require further investigation.

#### 1. Introduction

Oceanic oxygen availability significantly influences marine life and biogeochemical cycling, with changes in oxygenation associated with a range of biological and ecological effects (Breitburg et al., 2018). Regions with reduced oceanic oxygen content have been increasing globally in size since 1960 (Stramma et al., 2008; Schmidtko et al., 2017). Earth system models can project future oceanic oxygenation changes under possible global warming scenarios (e.g., Bopp et al. (2013); Fu et al. (2018)), and may be informed by studying the potential driving mechanisms of changes in oceanic oxygenation across past periods of climate change, including glacial-interglacial cycles (e.g., Galbraith and Jaccard (2015); Buchanan et al. (2016); Schmittner and Somes (2016); Yamamoto et al. (2019); Cliff et al. (2021)). However, a large uncertainty remains in the results of climate models, in part due to the lack of

reliable, quantitative paleo-O<sub>2</sub> data against which to validate model results (Yamamoto et al., 2019; Cliff et al., 2021).

Several (semi-)quantitative paleo-oxygenation proxies for glacial oceans have been proposed and calibrated to modern bottom-water oxygen (BWO) values. These proxies can be divided into two categories: (1) biological proxies: benthic foraminiferal species distributions and abundances (e.g., Sen Gupta and Machain-Castillo (1993); Bernhard and Sen Gupta (1999); Gooday (2003); Jorissen et al. (2007); Gooday et al. (2010); Erdem et al. (2020)), and the porosity or surface pore area percentages in benthic foraminiferal tests (e.g., Glock et al. (2011); Glock et al. (2012); Petersen et al. (2016); Tetard et al. (2017); Rathburn et al. (2018); Richirt et al. (2019); Tetard et al. (2021)); (2) geochemical proxies: redox-sensitive trace metals in bulk sediments such as V, Mo, U, Re, Mn, Fe (e.g., Morford and Emerson, 1999; Tribovillard et al., 2006; Bennett and Canfield, 2020); benthic foraminiferal carbon isotope

<sup>\*</sup> Corresponding author at: Department of Geology and Geophysics, Woods Hole Oceanographic Institution, Woods Hole, MA, USA. E-mail addresses: wlu@whoi.edu (W. Lu), catiafb@id.uff.br (C.F. Barbosa), arathburn@csub.edu (A.E. Rathburn), priscilamatta@id.uff.br (P.M. Xavier), acruz72@csub.edu (A.P.S. Cruz), ellen.thomas@yale.edu (E. Thomas), rosalind.rickaby@earth.ox.ac.uk (R.E.M. Rickaby), yige.zhang@tamu.edu (Y.G. Zhang), zunlilu@syr.edu (Z. Lu).

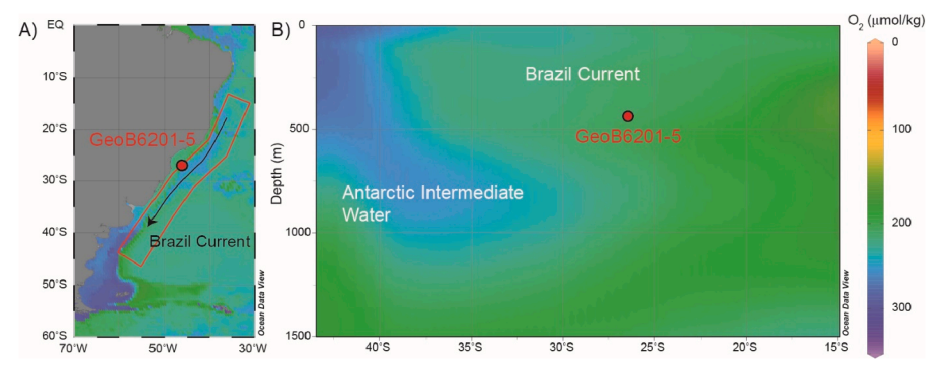


Fig. 1. Location of core GeoB6201–5. A) Modern bottom-water oxygen map for the Southwest Atlantic region. B). Depth profile (red box in A) showing well-oxygenated upper-intermediate waters on the southern Brazilian margin today. Figures are produced using the Ocean Data View software (Schlitzer, 2020), and O<sub>2</sub> data is from World Ocean Atlas 2018 (Garcia et al., 2018). (For interpretation of the references to colour in this figure legend, the reader is referred to the web version of this article.)

gradients ( $\Delta\delta^{13}$ C) between epifaunal (living on or above the seafloor surface) (*Cibicidoides wuellerstorfi*) and deep infaunal (living within sediments) species (*Globobulimina* spp.) (McCorkle and Emerson, 1988; Hoogakker et al., 2015; Hoogakker et al., 2018); preserved organic compounds (Anderson et al., 2019); and the I/Ca in benthic foraminiferal tests (Glock et al., 2014; Lu et al., 2020a).

Each paleo-O2 proxy has its own limitations and oxygen sensitivity window. Redox-sensitive trace metals are widely used to infer redox thresholds (e.g., oxic vs. anoxic, anoxic vs. euxinic) (Tribovillard et al., 2006; Bennett and Canfield, 2020). Benthic foraminiferal porosity, I/Ca, organic compound preservation, and benthic foraminiferal distribution proxies are most sensitive at low  $O_2$  ranges ( $< \sim 50 \mu \text{mol/kg}$ ), and may have larger uncertainties at higher O2 ranges (Rathburn et al., 2018; Anderson et al., 2019; Lu et al., 2020a; Erdem et al., 2020). The  $\Delta\delta^{13}$ C proxy is the only proxy calibrated to a wider O<sub>2</sub> range (20–235 µmol/ kg), but its application is limited due to the restricted common occurrence of the deep-infaunal, low-oxygen tolerant Globobulimina spp. (e.g., Jorissen et al. (2007)), the potential influence of seasonal phytodetrital flux on  $\delta^{13}C_{C. wuellerstorfi}$  (Mackensen et al., 1993), and the potential impact of anaerobic processes (including denitrification and sulfate reduction) on δ<sup>13</sup>C<sub>Globobulimina</sub> (McCorkle and Emerson, 1988; Piña-Ochoa et al., 2010a; Koho et al., 2013; Jacobel et al., 2020). A multiproxy approach, with independent proxy systematics and differing ranges of O<sub>2</sub> sensitivity, may provide more reliable paleo-O<sub>2</sub> estimates for the glacial oceans than a single proxy. Testing the consistency between new proxies in core-top and down-core samples is an important step towards quantitative proxy development. In this study, we focus on two recently developed proxies: benthic foraminiferal surface porosity and I/Ca.

In modern oceans, epifaunal foraminifera in low-oxygen waters tend to have a higher percentage of porosity on the dorsal side of their test (side that is exposed to bottom water) (e.g.,>15%) (Rathburn et al., 2018), likely due to the increased demand for gas exchange (Glock et al., 2012; Rathburn et al., 2018; Richirt et al., 2019). However, porosity will likely have an upper limit in order to sustain test robustness (Richirt et al., 2019). In contrast, tests of epifaunal foraminifera living in well-oxygenated waters (>200–250 µmol/kg) are likely to have fewer pores (e.g., < 5%), and may acquire oxygen mainly through the aperture (the primary opening in the test) (Rathburn et al., 2018). To date, the porosity in epifaunal foraminifera has not yet been tested as a recorder of paleo-oxygenation in down-core studies.

The I/Ca proxy has been calibrated on modern planktic and benthic foraminifera and applied in several studies over glacial-interglacial intervals (Lu et al., 2016; Hoogakker et al., 2018; Lu et al., 2019; Lu et al., 2020a; Lu et al., 2020b). The thermodynamically stable iodine species in seawater are mainly iodate (IO $_3$ -, oxidized form) and iodide (I-, reduced form), with minor dissolved organic iodine (Wong and Brewer, 1977; Luther III and Campbell, 1991; Ito and Hirokawa, 2009). Iodate is completely reduced to iodide under anoxic conditions (no O $_2$ ), and iodide is re-oxidized to iodate when oxygen increases (Rue et al., 1997). Only iodate can be incorporated into the calcite structure (Lu et al.,

2010) by replacing the carbonate ion (Podder et al., 2017; Feng and Redfern, 2018). Therefore, lower foraminiferal I/Ca values generally indicate less-oxygenated conditions. The combination of low epifaunal I/Ca values (<~3 µmol/mol) and independent oxygenation proxies has been argued to be more reliable to detect low-oxygen waters in glacial oceans than the use of a single proxy (Lu et al., 2020a).

In this study, we apply the epifaunal benthic foraminiferal surface porosity proxy and the I/Ca proxy to foraminifera from a core (GeoB6201-5) on the southern Brazilian margin. This study presents the first application of the porosity proxy in epifaunal fossil foraminifera, and we directly compare the porosity with I/Ca values to evaluate proxy potentials and limitations.

## 2. Samples and methods

#### 2.1. Study site

Core GeoB6201–5 (26°40.22′S, 46°26.46′W, 475 m water depth; 247 cm long) was taken on the upper slope of the Brazilian margin, below the southward path of the Brazil Current (Schulz et al., 2001), a location presently bathed by well-oxygenated waters (BWO of ~225  $\mu$ mol/kg) (Schulz et al., 2001; Garcia et al., 2018) (Fig. 1). Anomalously negative  $\delta^{13}$ C values of glacial foraminifera in this core (Portilho-Ramos et al., 2018) and the occurrence of authigenic carbonate nodules with low  $\delta^{13}$ C values (down to -30%) in glacial samples from nearby cores (Kowsmann and de Carvalho, 2002; Wirsig et al., 2012) have been interpreted as indicating that methane seeps may have been active for thousands of years on the southern Brazilian margin.

## 2.2. Age model

The age model follows Portilho-Ramos et al. (2018) and is based on (1) six accelerator mass spectrometry (AMS)  $^{14}$ C ages on the planktic foraminifer *Globigerinoides ruber*. Samples were selected at levels without anomalously negative  $\delta^{13}$ C values (except for the basal age of 235 cm). The age model and associated uncertainty were calculated using the BACON model and the IntCal13 calibration curve with a reservoir correction of  $400 \pm 100$  years {Blaauw and Christen, 2011 #72}(Blaauw and Christen, 2011; Reimer et al., 2013); (2) comparison of the *Cibicidoides* spp.  $\delta^{18}$ O record with that of adjacent, well-dated core GeoB2107–3 (27°10'S, 46°27'W, 1048 m water depth) (Gu et al., 2017; Hendry et al., 2012) and the regional, intermediate-depth South Atlantic benthic  $\delta^{18}$ O stack (Lisiecki and Stern, 2016). (3) comparison of abundance changes of the planktic foraminiferal species *Globorotalia menardii* and *Globorotalia inflata*, indicative of glacial-interglacial biozones (Ericson and Wollin, 1968).

## 2.3. Foraminiferal surface porosity analyses

Specimens of the benthic foraminiferal species *C. wuellerstorfi* and *Cibicidoides pseudoungerianus* were picked from the size fraction >150

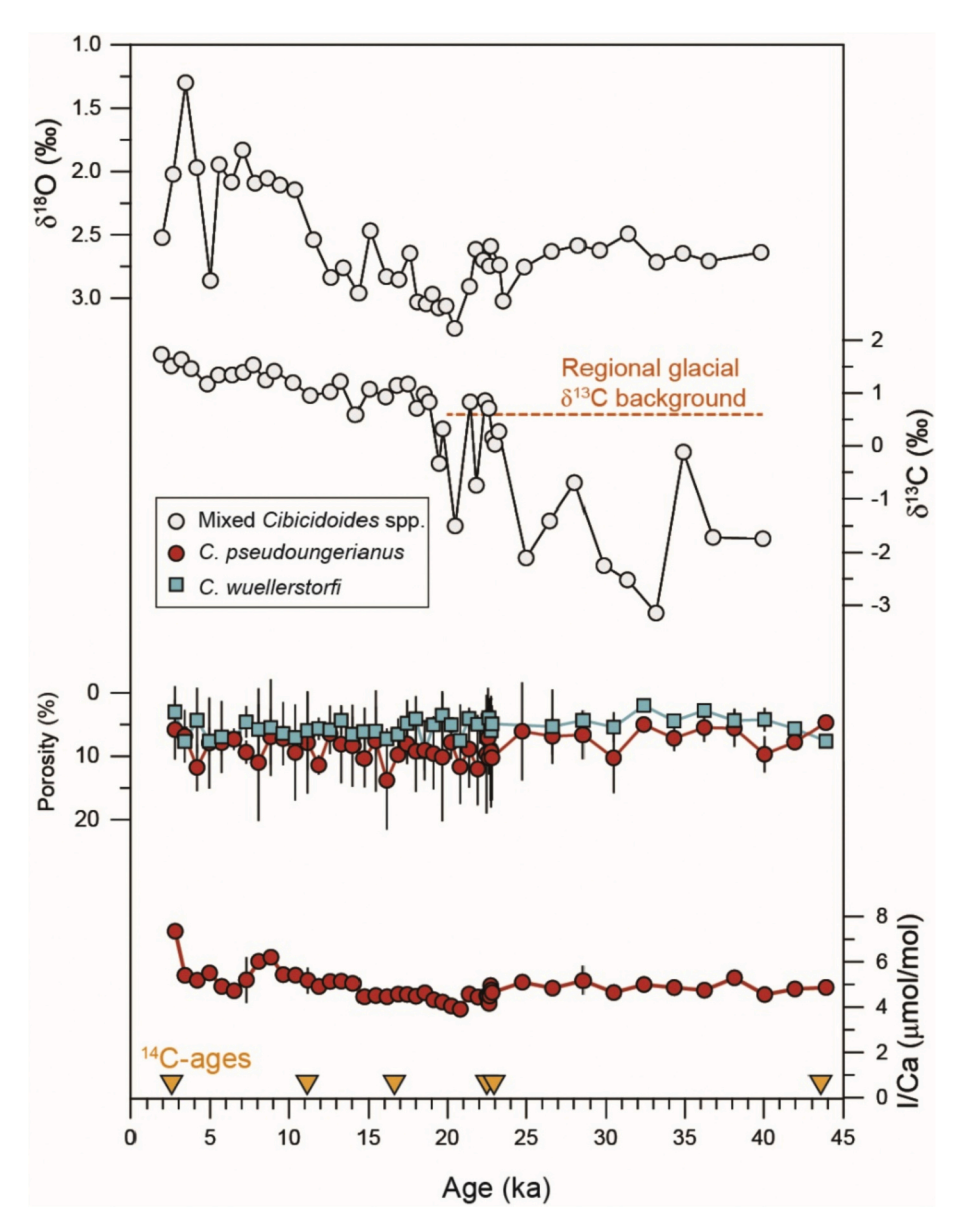


Fig. 2. Benthic foraminiferal porosity and I/Ca records from core GeoB6201–5 (this study) along with benthic  $\delta^{18}O$  and  $\delta^{13}C$  records for the same core (Portilho-Ramos et al., 2018). The error bars are  $2\sigma$ ; note that some porosity samples were measured on only one specimen (Table S2) and some error bars in porosity are smaller than the symbol sizes.

μm at a sampling resolution of 5 cm. We measured and calculated surface porosity of benthic foraminifera following Petersen et al. (2016).

For each sampling depth, three to four well-preserved specimens of each species (i.e., with a whole test without significant dissolution or loss, although the last chamber is commonly broken or absent) were analyzed, for a total of 275 individuals in 48 samples. Some samples do not have three well-preserved specimens, so one or two individuals were used. Photomicrographs were made using a Scanning Electron Microscope (SEM), Hitachi model TM3000. The dorsal side of each specimen was imaged at 300× magnification using the same scale for comparison. The SEM images underwent a first correction and editing in Adobe Photoshop. ImageJ, a semi-automatic software, was then used to calculate the pore areas in the penultimate chamber, based on a gray-scale threshold applied to a specific frame. Frames were manually positioned using a macro (Petersen et al., 2016) that allowed us to place a frame of a fixed size on the SEM images. Some adjustments were made in the macro due to the image magnification (300×) used here, rather

than the 1000× used by Petersen et al. (2016).

Five different frame sizes with different proportions were first tested to select the frame that best represented the porosity of the chambers. The frame sizes were tested initially for top, middle and bottom of the core, then afterwards applied to the rest of the core. A non-parametric analysis (Kolmogorov-Smirnov-KS) using R-software was carried out on the pore area data of five different frames to test the distribution of the data, helping to determine which frame would be the most suitable for the species used (Table S1). Subsequently, the same fixed frame size (Frame 1 with 124  $\mu m \times 64~\mu m)$  was applied to all 271 microphotographs analyzed. The porosity of each specimen was used to determine the average (typically of three individuals) for each sample. Standard Deviations (S.D.) of porosity are reported for each sample (Table S2).

## 2.4. Foraminiferal I/Ca analyses

After the porosity measurements were completed, I/Ca analyses

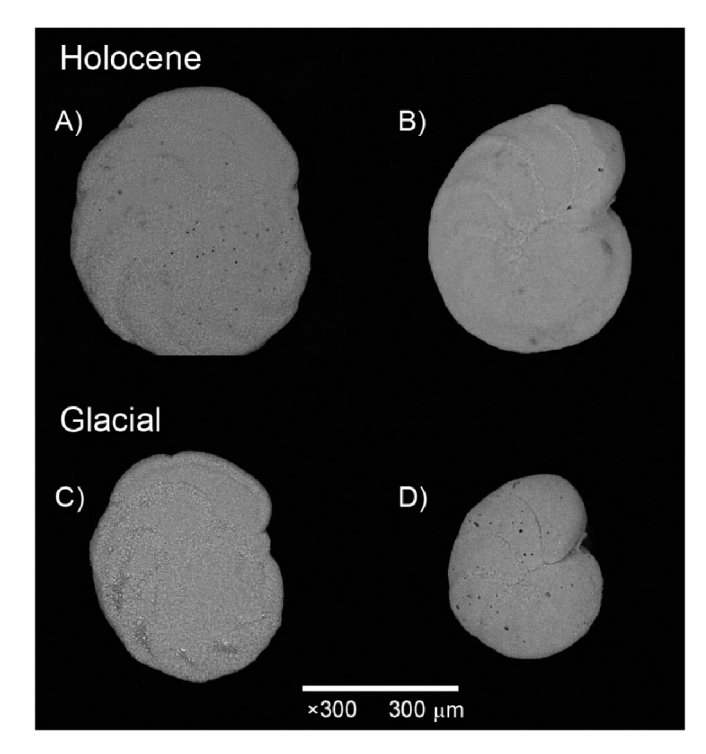


**Fig. 3.** SEM images of selected Holocene and glacial benthic foraminifera. A) *C. wuellerstorfi* at 15 cm depth. B) *C. pseudoungerianus* at 35 cm depth. C). *C. wuellerstorfi* at 120 cm depth. D) *C. pseudoungerianus* at 210 cm depth.

were performed on the same set of specimens, following Lu et al. (2020a). About 10 specimens of benthic foraminifera are typically required for I/Ca analyses on an ICP-MS in order to reduce analytical uncertainty due to small sample size. Around 15 specimens of C. pseudoungerianus were used for each sampling depth (5 cm). The foraminiferal cleaning method followed the Mg/Ca protocol of Barker et al. (2003). The samples were gently crushed using cleaned glass slides to open all chambers. Samples were then cleaned by ultrasonication in de-ionized water to remove clays, a 10-min boiling-water bath in NaOHbuffered 1% H<sub>2</sub>O<sub>2</sub> solutions to remove organic matter, and three additional rinses with de-ionized water. The oxidative cleaning step is required because I/Ca in uncleaned specimens can be 10 to 1000 times higher than in cleaned samples, due to organic-associated iodine (Glock et al., 2016, 2019). The cleaned samples were dissolved in 3% HNO<sub>3</sub>, then diluted to solutions containing ~50 ppm Ca, internal standards (5 ppb In and Cs), and 0.5% tertiary amine (to stabilize iodine). The measurements were performed immediately on a quadrupole ICP-MS (Bruker M90) at Syracuse University. Calibration standards were freshly made for each batch of samples. The sensitivity of iodine is tuned to  $\sim\!90$  kcps for 1 ppb standard, and the standard deviation for three blanks in a row is  $<\!1$  kcps. The precision for  $^{127}I$  is typically better than 1%. The reference standard JCp-1 was analyzed between each 3 unknown samples (I/Ca raw value of  $3.98\pm0.15~\mu\text{mol/mol}$  (n=17) for all batches) to monitor long-term accuracy (I/Ca reference value of 4.27  $\mu\text{mol/mol}$ ) (Lu et al., 2010; Lu et al., 2020b). The detection limit of I/Ca is on the order of 0.1  $\mu\text{mol/mol}$ . Replicates of selected samples from glacial and interglacial intervals yielded a reproducibility ranging from  $\pm0.004~\mu\text{mol/mol}$  (2 $\sigma$ ) to  $\pm0.98~\mu\text{mol/mol}$  (2 $\sigma$ ) for I/Ca (Table S2).

## 2.5. Benthic foraminiferal habitat

Epifaunal to shallow infaunal foraminifera are thought to record bottom-water conditions above the sediment-water interface, in contrast to deeper infaunal species, which reflect pore water conditions (e.g., McCorkle and Emerson (1988); Mackensen (2008); Hoogakker et al. (2015)). Cibicidoides wuellerstorfi is an epifaunal species, commonly attached to objects projecting above the sediment-water interface (Lutze and Thiel, 1989; Rathburn and Corliss, 1994). This species has been found in abundance in well-oxygenated environments, but also in low-O<sub>2</sub> settings (Burkett et al., 2016; Rathburn et al., 2018; Venturelli et al., 2018). Cibicidoides pseudoungerianus, also used in this study, is taxonomically not as well-defined, morphologically close to Cibicidoides pachyderma (Schweizer, 2006), and thought to be a synonym of the latter by some authors (e.g., Altenbach et al. (2003); Licari and Mackensen (2005)). Cibicidoides pseudoungerianus typically occurs on the deep and upper continental slope (< 2000 m), in areas with a broad range of organic carbon fluxes and primary productivity (Altenbach et al., 1999, 2003). It has been described as epifaunal, attached to hard substrates such as hydroids (Dobson and Haynes, 1973; Brasier, 1975), and as shallow infauna dwelling at between +1 and -1 cm of the sedimentwater interface (Schweizer, 2006).

## 3. Results

The porosity down-core values average 5.5% for *C. wuellerstorfi* (n=47, S.D. =1.4%) and 8.5% for *C. pseudoungerianus* (n=48, S.D. =2.0%), and the I/Ca values average 4.9 µmol/mol for *C. pseudoungerianus* (n=48, S.D. =0.6 µmol/mol) (Figs. 2 and 3, Supplementary Table S2). Average porosity values in each species are similar in sediments deposited during the Holocene (0-10 ka, n=10), deglaciation (10-18 ka, n=12) and the last glacial period (18-45 ka, n=26) (averages 5.9%, 5.9%, and 5.1% respectively for *C. wuellerstorfi*; averages 8.2%, 9.2% and 8.3% respectively for *C. pseudoungerianus*) (Fig. 4). The I/Ca values average 5.6 µmol/mol during the Holocene, with similar values during the deglaciation and the last glacial period (averages 4.8 and 4.6 µmol/mol, respectively) (Fig. 4).

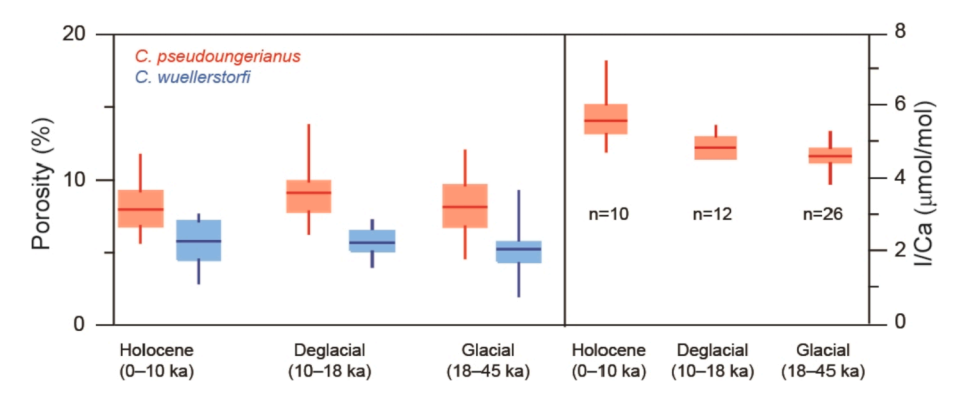


Fig. 4. Candlestick plot for porosity and I/Ca from core GeoB6201–5. The red box marks the 25th and 75th percentiles, the red horizontal line inside the box indicates the average, and the whiskers show the maximum and minimum values. (For interpretation of the references to colour in this figure legend, the reader is referred to the web version of this article.)

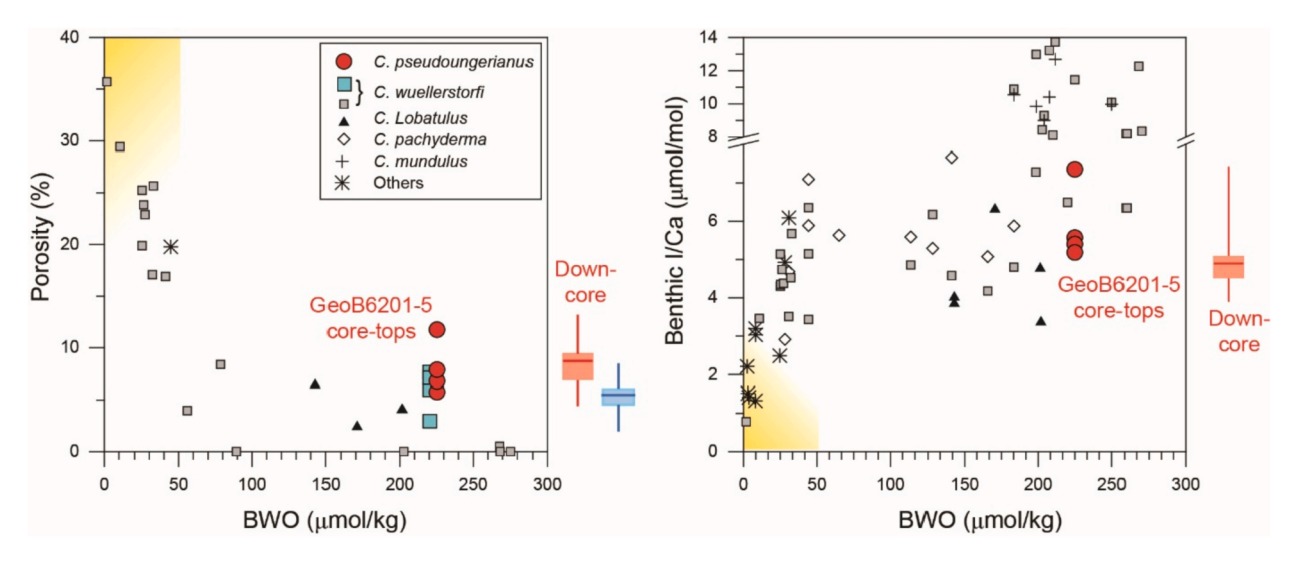


Fig. 5. Comparison of core-top foraminiferal porosity and I/Ca (ages <5 ka) in core GeoB6201–5 (this study) with global calibration dataset (Rathburn et al., 2018; Lu et al., 2020a). The box marks the 25th and 75th percentiles in the GeoB6201–5 down-core record, the horizontal line inside the box indicates the average, and the whiskers show the maximum and minimum values. Yellow shaded areas show the low-O<sub>2</sub> thresholds as proposed in Lu et al. (2020a). The porosity calibration dataset from Rathburn et al. (2018) represents average values of multiple specimens at each location. (For interpretation of the references to colour in this figure legend, the reader is referred to the web version of this article.)

Core-top benthic foraminiferal porosity and I/Ca values in core GeoB6201–5 (ages <5 ka) agree well with the values in the global core-top dataset of porosity and I/Ca values (Fig. 5) (Rathburn et al., 2018; Lu et al., 2020a). The porosity values in *C. pseudoungerianus* are generally higher than those in *C. wuellerstorfi* throughout the record, probably because *C. pseudoungerianus* is partly influenced by pore water conditions or because there are species-specific differences in oxygen requirements or in the calcification process. Most porosity and I/Ca proxy records (as represented by the 25th and 75th percentile values) in core GeoB6201–5 fall into the data range corresponding to modern BWO in the core-top data set, i.e., between 50 and 250 µmol/kg (Fig. 5).

We used the two-group Mann-Whitney test (a nonparametric test that allows two groups to be compared without making the assumption that values are normally distributed) to evaluate whether the porosity and I/Ca values changed significantly across different climate states (Holocene vs. deglaciation vs. last glacial period). Porosity values are not significantly different in Holocene vs. deglacial (p=0.87 for C. wuellerstorfi, p=0.14 for C. pseudoungerianus), or in deglacial vs. glacial (p=0.07 for C. wuellerstorfi, p=0.29 for C. pseudoungerianus). I/Ca values are significantly different in Holocene vs. deglacial (p<0.01), but not in deglacial vs. glacial (p=0.19). These variations may not necessarily indicate changes in BWO, because modern calibration data suggest both I/Ca and porosity proxies are not linearly sensitive to  $O_2$  changes between 50 and 250 µmol/kg (Section 4.2).

## 4. Discussion

## 4.1. Potential influence of authigenic carbonate

The presence of high-Mg calcite and elevated Mg and S concentrations in some (but not all) glacial samples in core GeoB6201–5 suggest overgrowths of post-depositional authigenic carbonate induced by anaerobic oxidation of methane, possibly related to the anomalously negative  $\delta^{13} \text{C}$  values in some samples (Portilho-Ramos et al., 2018). Authigenic carbonate precipitation in marine anoxic pore-waters is expected to lower I/Ca values (Hardisty et al., 2017), because the reduced species  $\text{I}^-$  is the only iodine speciation in anoxic pore fluids and will not be incorporated into calcite (Lu et al., 2010). We examined the potential effects of authigenic carbonate overgrowths on our records by comparing the porosity and I/Ca data in glacial samples with high-Mg calcite vs. those without high-Mg calcite (between 140 and 235 cm

core depth) (Fig. 6A, Supplementary Tables S3). We did not find consistent or systematic differences in porosity or I/Ca between samples with and without high-Mg calcite. Porosity and I/Ca values from glacial samples with anomalously negative  $\delta^{13}$ C values (whether the isotopic signal was affected by authigenic overgrowths or not) were similar to those from samples without anomalous values (Fig. 6B). This similarity in porosity and I/Ca values, together with a lack of evidence of surface overgrowths in SEM images of tests examined in this study, indicates that authigenic carbonate overgrowths probably did not significantly affect the porosity and I/Ca signals.

## 4.2. Comparing porosity and I/Ca

The porosity and I/Ca calibrations were developed using epifaunal C. wuellerstorfi. Ideally, down-core applications should use epifaunal species to eliminate the potential influence of pore-water conditions. However, when epifaunal species are not available in sufficient numbers for I/Ca analyses, shallow infaunal Cibicidoides species may provide paleo-O<sub>2</sub> information. For example, core-top shallow infaunal species (e. g., C. pachyderma and C. mundulus) had I/Ca values similar to those in C. wuellerstorfi at the same locations (Lu et al., 2020a). As another example, in a down-core record from the Eastern Equatorial Pacific, I/Ca trends of C. wuellerstorfi and C. pachyderma over the last 45 kyr are similar, both ranging between 0 and  $\sim$  6  $\mu$ mol/mol (Lu et al., 2020a). The temporal trends of porosity in both C. pseudoungerianus and C. wuellerstorfi are similar (Fig. 2), suggesting that they respond similarly to oxygenation changes. Hence, we posit that porosity changes in C. pseudoungerianus are not completely due to its potential shallow infaunal habitat, and that both Cibicidoides species likely recorded BWO

A combination of low I/Ca (< 3 µmol/mol) and high porosity (> 15%) can indicate low- $O_2$  waters (Lu et al., 2020a). We cannot be certain that BWO conditions did not change over the last 45 kyr at the core site studied here, because of the large uncertainty in oxygenation values derived from the modern calibration (50–250 µmol/kg) (Fig. 5). The I/Ca proxy sensitivity to low- $O_2$  waters is possibly related to modern ocean iodine geochemistry: low iodate concentrations (<0.15 µmol/L) are found in low- $O_2$  waters only, whereas high iodate concentrations are associated with a wide range of  $O_2$  concentrations (Lu et al., 2019; Hardisty et al., 2021).

The sensitivity of the porosity proxy is related to poorly known pore

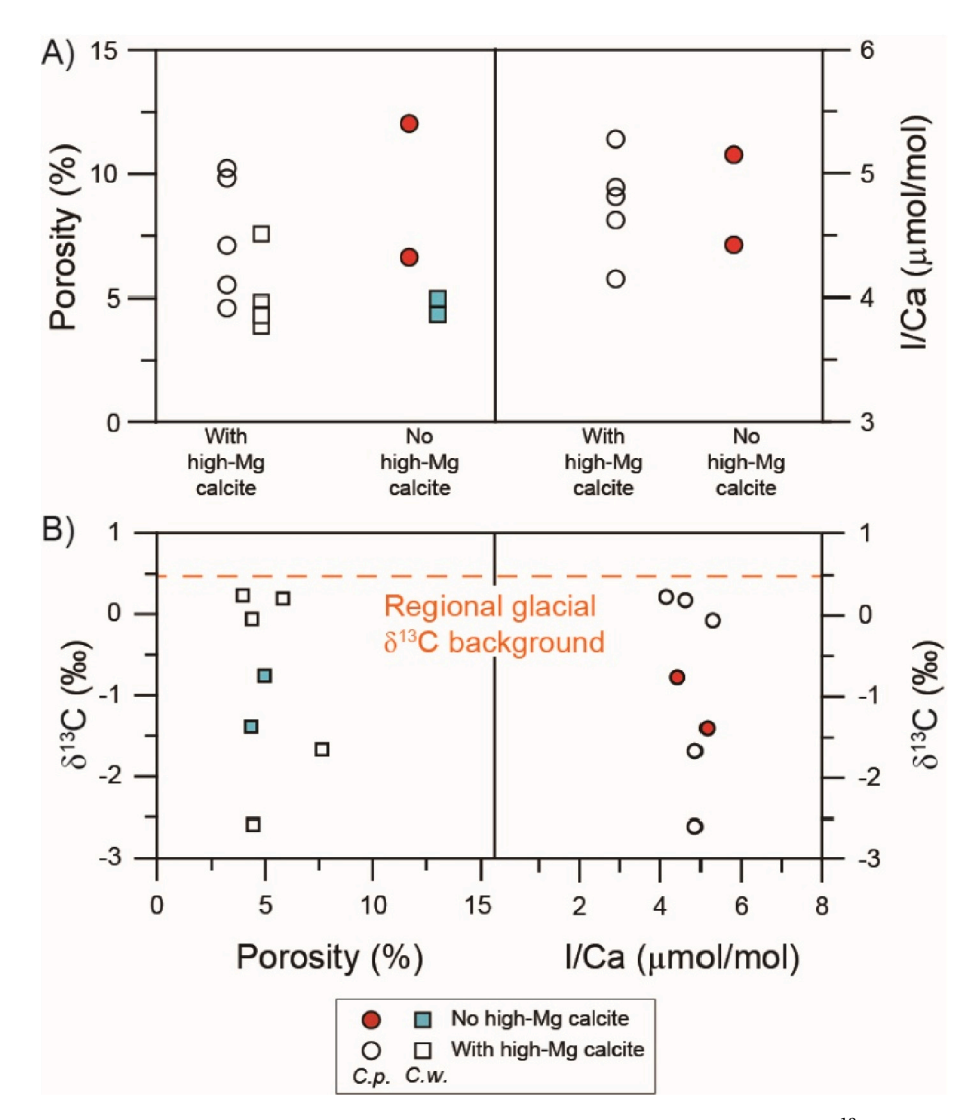


Fig. 6. A) Comparison of porosity and I/Ca in glacial samples with and without high-Mg calcite. B) Cross plot of glacial  $\delta^{13}C_{C.\ wuellerstorfl}$  vs. porosity and I/Ca. The identification of high-Mg calcite is based on bulk sediment mineralogy and Mg contents (Portilho-Ramos et al., 2018).

functions of foraminifera: below the low- $O_2$  threshold, epifaunal foraminifera will probably need to adjust their pore size and volume (= porosity) to obtain sufficient oxygen, whereas above this threshold, they do not require pores to be used in respiration, and can mainly respire through the aperture (Rathburn et al., 2018). The causes of variability in porosity and I/Ca at  $O_2$  levels between 50 and 250  $\mu$ mol/kg remain unclear.

We thus suggest that the glacial BWO at the location of core GeoB6201–5 was most likely above the threshold of 50  $\mu$ mol/kg over the full time represented in the core. This suggestion agrees with the results of modeling studies indicating that O<sub>2</sub> values at ~500 m water depths at ~27°S in the South Atlantic Ocean during the LGM were not significantly different from those in pre-industrial times (Schmittner and Somes, 2016; Yamamoto et al., 2019; Cliff et al., 2021). The mechanisms stabilizing BWO may be related to relatively stable oceanographic conditions during the last glacial period, or to competing effects of ocean stratification (thus ventilation) and productivity (thus O<sub>2</sub> utilization) during LGM and Heinrich Stadial 1 in the region (Pereira et al., 2018).

## 4.3. Potential non-O2 factors

Both porosity and I/Ca proxies can be used to provide paleo-O2

information, but other (non-O<sub>2</sub>) factors may influence these proxies (Glock et al., 2012, 2014; Rathburn et al., 2018; Richirt et al., 2019; Lu et al., 2020a). Below, we attempt to explore how these potential factors may affect the proxies.

## 4.3.1. I/Ca proxy

To better understand the I/Ca proxy systematics, we must establish the mechanistic relationship between seawater iodate and O2 before making the connection to foraminiferal I/Ca in modern samples. However, the relationship between seawater iodate and O2 is currently not well understood, and may vary on regional/temporal scales. No seawater iodate data are available in the studied region. The reduction of iodate to iodide may occur rapidly in low-O2 waters (Chance et al., 2014). The  $O_2$  threshold for iodate reduction was reported to be  $\sim 10$ μmol/kg in the Pacific Ocean (Rue et al., 1997; Huang et al., 2005) and Arabian Sea (Farrenkopf and Luther Iii, 2002), but it was higher (< ~70–100 µmol/kg) in the Benguela upwelling region in the Southeast Atlantic (Chapman, 1983). Iodate reduction rates may vary spatially, possibly driven by the availability of organic carbon, sulfide, and nitrite, which may have been involved in iodate reduction processes (Hardisty et al., 2021). Other regional processes, such as water mass ages, may also cause spatial iodate variability in different marine settings (Hardisty

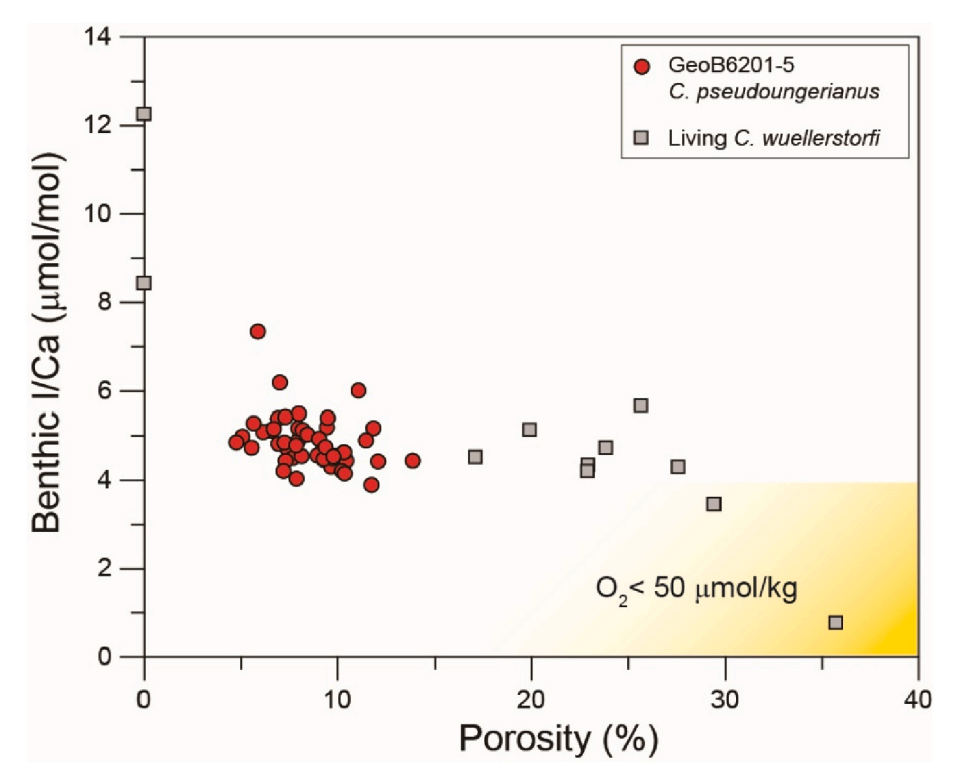


Fig. 7. Cross-plot of porosity and benthic I/Ca in living *C. wuellerstorfi* (Rathburn et al., 2018; Lu et al., 2020a) and GeoB6201–5*C. pseudoungerianus*. Note that porosity and I/Ca were measured on the same set of specimens. Yellow shaded areas show the low-O<sub>2</sub> thresholds in Fig. 5. (For interpretation of the references to colour in this figure legend, the reader is referred to the web version of this article.)

#### et al., 2021).

The reverse process (iodide re-oxidation to iodate) may also play a role in affecting the seawater iodate concentrations, thus foraminiferal I/Ca. The kinetics of iodide re-oxidation have been suggested to be slow, ranging from months to decades (Chance et al., 2014). The I/Ca signals in samples across the deglaciation in the Eastern Equatorial Pacific may have been affected by a slow increase in O2 (recovery from depleted glacial values) at some upstream locations (Lu et al., 2020a). However, in the studied core we did not find large changes in I/Ca or porosity during deglaciation, consistent with the occurrence of relatively constant O<sub>2</sub> in upstream waters, between the equator and 25°S, during the LGM, as seen in model simulations (Schmittner and Somes, 2016; Yamamoto et al., 2019; Cliff et al., 2021). The combination of lateral and vertical diffusion/advection of low iodate waters from nearby locations and slow iodide re-oxidation kinetics could complicate foraminiferal I/ Ca records, which thus might not reflect in-situ O<sub>2</sub> (Lu et al., 2019; Hardisty et al., 2021). The studied region of the southern Brazilian margin is currently bathed in well-oxygenated waters without large spatial O<sub>2</sub> variations being observed (Schulz et al., 2001; Garcia et al., 2018). Water mass mixing thus probably does not have a major impact on benthic I/Ca in this region.

Trace elemental ratios in foraminifera are commonly thought to be impacted by environmental parameters such as temperature and carbonate ion concentrations. Temperature might have a negative impact on the iodine partition coefficient in laboratory synthesized calcite experiments: I/Ca may decrease at higher temperatures while other variables remain constant (Zhou et al., 2014). The negative temperature impact would have resulted in higher I/Ca values during the LGM, but we did not observe this. It is unclear how much effect temperature and other environmental factors (e.g., salinity, carbonate saturation states, and pH) can have on foraminiferal I/Ca, and this will be the subject of ongoing research.

## 4.3.2. Porosity proxy

The functions of dorsal pores on benthic foraminiferal tests are not fully understood. It has been suggested that pores can be used in gas exchange and taking up dissolved organic materials, but their functions may differ between species (Glock et al., 2012). Other than O<sub>2</sub> acquisition, the pores may also be used to transport respiratory products such as CO<sub>2</sub>, although it remains unclear whether or how this process could impact the porosity. Higher porosity can be due to higher pore density (number of pores per surface area) and/or greater pore size (Petersen et al., 2016), or increasing pore size but simultaneously decreasing pore density (Richirt et al., 2019). Pore size and pore density in foraminiferal tests are likely interdependent (Richirt et al., 2019), and porosity takes both variables into account, thus likely representing the individual foraminifer's oxygen accessibility better than either pore density or pore diameter alone (Rathburn et al., 2018).

Mechanical constraints (shell robustness) may limit foraminiferal pore patterns (Richirt et al., 2019). *Ammonia*, a common cosmopolitan intertidal infaunal genus (Hayward et al., 2021), has an upper porosity limit of 30%, probably due to mechanical constraints (Richirt et al., 2019), but living epifaunal *C. wuellerstorfi* has a porosity up to 50% in low- $O_2$  waters (10.7  $\mu$ mol/kg) at a Northwest Pacific site (Rathburn et al., 2018). Thinner-walled tests (thus possibly faster gas exchange) may be an alternative way for foraminifera to adapt to  $O_2$ -depleted environments (Bernhard, 1986; Kaiho, 1994), but quantitative measurements of test robustness have not been established, and the relations between shell robustness and  $O_2$  needs further investigation in paleoceanographically-important taxa.

Previous studies linked pore sizes and/or pore density in different species of infaunal foraminifera to ambient conditions, i.e., BWO and bottom-water nitrate concentrations (e.g., (Glock et al., 2011; Glock et al., 2012; Kuhnt et al., 2013; Kuhnt et al., 2014)). Many infaunal foraminiferal taxa store and respire nitrate to survive under anoxic conditions (Risgaard-Petersen et al., 2006; Piña-Ochoa et al., 2010a;

Piña-Ochoa et al., 2010b; Bernhard et al., 2012), and denitrification is an important metabolic mechanism that enables some species to survive in anoxic conditions (Piña-Ochoa et al., 2010a). The pore density in infaunal *Bolivina spissa* correlates to bottom-water nitrate concentrations (Glock et al., 2011), and has been used to reconstruct deglacial nitrogen inventory changes in the Peruvian upwelling region (Glock et al., 2018).

In contrast to these infaunal species, the epifaunal or shallow infaunal *Cibicidoides* spp. typically do not migrate to anoxic waters deeper in the sediments, thus probably do not use nitrate for respiration (Rathburn et al., 2018). *Cibicidoides pachyderma* was observed not to use nitrate (Piña-Ochoa et al., 2010a). In conclusion, oxygen availability influences porosity in epifaunal benthic foraminifera (Rathburn et al., 2018), but other factors such as respiratory products, shell robustness (Richirt et al., 2019) and morphometrics (i.e., major axis and roundness) (Tetard et al., 2021) may play a role, and need additional investigation.

## 4.4. Study limitations and suggestions for future proxy developments

We suggest that the benthic foraminiferal porosity proxy and the benthic I/Ca proxy are generally consistent in our down-core record. The development of both proxies started only recently, thus there is only a limited amount of data from living *C. wuellerstorfi*, insufficient to show how well the two proxies relate to each other in the same set of specimens (Fig. 7). We explore this relationship by including down-core data from core GeoB6201–5, which are not significantly different from those of living *C. wuellerstorfi*, with values clustering in the middle range (2–10% for porosity; 4–7 µmol/mol for I/Ca). Living *C. wuellerstorfi* reflect a much wider  $O_2$  range, from 2 to 277 µmol/kg, than the downcore samples. The overall correlation between I/Ca and porosity is not strong when considering all data points. Both proxies appear to show threshold behavior with  $O_2$  rather than a linear correlation; there are limited samples of the two endmember (porosity <5% and > 15%) ranges, and only two *Cibicidoides* spp. were measured.

For future proxy developments, we recommend three general directions: (1) coupled seawater  $O_2$ , iodate, iodide, foraminiferal I/Ca, porosity, shell morphometrics, shell robustness (if possible) measurements, ideally combined with pore-water profiles in a range of oceanographic regions to better understand the proxy systematics; (2) obtain more live-collected or core-top samples with high porosity - low I/Ca to better define the low  $O_2$  endmember and test correlations; (3) work on regional calibrations to better evaluate the potential effect of non- $O_2$  factors on both proxies under similar  $O_2$  conditions.

## 5. Conclusions

The close correspondence between porosity and I/Ca proxies in a down-core record from the southern Brazilian margin over the last 45 kyr builds confidence in the combined use of these proxies to reconstruct past changes in oceanic  $O_2$ . We infer that the BWO at the location of core GeoB6201–5 likely remained above  $\sim 50~\mu mol/kg$  over the last glacial period, but a more precise  $O_2$  estimate cannot be made due to the uncertainties of both proxies in higher  $O_2$  windows. Our current understanding of both proxies is still incomplete, and more work is required to better understand the proxy systematics and potential influencing factors. Both proxies are fundamentally different from other paleo- $O_2$  proxies (i.e., redox-sensitive trace metals, carbon isotope gradients, organic compounds, and foraminiferal assemblages), and are based on widely-distributed benthic species, thus may have the potential to be applied in broad regions, and provide independent reconstructions of  $O_2$  conditions.

## **Declaration of Competing Interest**

The authors declare that they have no known competing financial interests or personal relationships that could have appeared to influence the work reported in this paper.

#### Acknowledgements

We thank the Bremen Core Repository for curating and providing material from core GeoB6201–5. This work is supported by NSF grants OCE-1232620, OCE-1736542, and EAR-1349252 (to ZL), OCE 10–60,992 (to AER), and OCE 1736538 (to ET). CFB thanks Coordenação de Aperfeiçoamento de Pessoal de Nível Superior – Brazil (CAPES) – Finance Code 001. All data are publicly available as supporting information to this document, and through doi:https://doi.org/10.1594/PANGAEA.914577.

## Appendix A. Supplementary data

Supplementary data to this article can be found online at https://doi.org/10.1016/j.palaeo.2021.110588.

#### References

- Altenbach, A.V., Pflaumann, U., Schiebel, R., Thies, A., Timm, S., Trauth, M., 1999. Scaling percentages and distributional patterns of benthic foraminifera with flux rates of organic carbon. J. Foraminiferal Res. 29, 173–185.
- Altenbach, A.V., Lutze, G.F., Schiebel, R., Schönfeld, J., 2003. Impact of interrelated and interdependent ecological controls on benthic foraminifera: an example from the Gulf of Guinea. Palaeogeogr. Palaeoclimatol. Palaeoecol. 197, 213–238.
- Anderson, R.F., Sachs, J.P., Fleisher, M.Q., Allen, K.A., Yu, J., Koutavas, A., Jaccard, S.L., 2019. Deep-sea oxygen depletion and ocean carbon sequestration during the last ice age. Glob. Biogeochem. Cycles 33, 1–17.
- Barker, S., Greaves, M., Elderfield, H., 2003. A study of cleaning procedures used for foraminiferal Mg/Ca paleothermometry. Geochem. Geophys. Geosyst. 4 (9).
- Bennett, W.W., Canfield, D.E., 2020. Redox-sensitive trace metals as paleoredox proxies: a review and analysis of data from modern sediments. Earth Sci. Rev. 204, 103175.
- Bernhard, J.M., 1986. Characteristic assemblages and morphologies of benthic foraminifera from anoxic, organic-rich deposits; Jurassic through Holocene. J. Foraminifer. Res. 16 (3), 207–215.
- Bernhard, J.H., Sen Gupta, B.K., 1999. Foraminifera in oxygen-depleted environments. In: Gupta, S. (Ed.), Modern Foraminifera. Springer, Dordrecht, pp. 201–216.
- Bernhard, J.M., Casciotti, K.L., McIlvin, M.R., Beaudoin, D.J., Visscher, P.T., Edgcomb, V. P., 2012. Potential importance of physiologically diverse benthic foraminifera in sedimentary nitrate storage and respiration. J. Geophys. Res. Biogeosci. 117 (G3).
- Blaauw, M., Christen, J.A., 2011. Flexible paleoclimate age-depth models using an autoregressive gamma process. Bayesian Anal. 6 (3), 457–474.
- Bopp, L., Resplandy, L., Orr, J.C., Doney, S.C., Dunne, J.P., Gehlen, M., Halloran, P., Heinze, C., Ilyina, T., Séférian, R., Tjiputra, J., Vichi, M., 2013. Multiple stressors of ocean ecosystems in the 21st century: projections with CMIP5 models. Biogeosciences 10, 6225–6245.
- Brasier, M.D., 1975. The ecology and distribution of recent foraminifera from the reefs and shoals around Barbuda, West Indies. J. Foraminiferal Res. 5, 193–210.
- Breitburg, D., Levin, L.A., Oschlies, A., Grégoire, M., Chavez, F.P., Conley, D.J., Garçon, V., Gilbert, D., Gutiérrez, D., Isensee, K., et al., 2018. Declining oxygen in the global ocean and coastal waters. Science 359, eaam7240.
- Buchanan, P.J., Matear, R.J., Lenton, A., Phipps, S.J., Chase, Z., Etheridge, D.M., 2016. The simulated climate of the last glacial maximum and insights into the global marine carbon cycle. Clim. Past 12, 2271–2295.
- Burkett, A.M., Rathburn, A.E., Pérez, M.E., Levin, L.A., Martin, J.B., 2016. Colonization of over a thousand Cibicidoides wuellerstorfi (foraminifera: Schwager, 1866) on artificial substrates in seep and adjacent off-seep locations in dysoxic, deep-sea environments. Deep-Sea Res. I Oceanogr. Res. Pap. 117, 39–50.
- Chance, R., Baker, A.R., Carpenter, L., Jickells, T.D., 2014. The distribution of iodide at the sea surface. Environ Sci Process Impacts 16 (8), 1841–1859.
- Chapman, P., 1983. Changes in iodine speciation in the Benguela current upwelling system. Deep Sea Res. Part A. Oceanogr. Res. Pap. 30 (12), 1247–1259.
- Cliff, E., Khatiwala, S., Schmittner, A., 2021. Glacial deep ocean deoxygenation driven by biologically mediated air–sea disequilibrium. Nat. Geosci. https://doi.org/10.1038/ s41561-020-00667-z.
- Dobson, M., Haynes, J., 1973. Association of foraminifera with hydroids on the deep shelf. Micropaleontology 19, 78–90.
- Erdem, Z., Schönfeld, J., Rathburn, A.E., Pérez, M.E., Cardich, J., Glock, N., 2020.
  Bottom-water deoxygenation at the Peruvian margin during the last deglaciation recorded by benthic foraminifera. Biogeosciences 17, 3165–3182.
- Ericson, D.B., Wollin, G., 1968. Pleistocene climates and chronology in deep-sea sediments. Science 162 (3859), 1227–1234.
- Farrenkopf, A.M., Luther Iii, G.W., 2002. Iodine chemistry reflects productivity and denitrification in the Arabian Sea: evidence for flux of dissolved species from sediments of western India into the OMZ. Deep-Sea Res. II Top. Stud. Oceanogr. 49 (12), 2303–2318.
- Feng, X., Redfern, S.A., 2018. Iodate in calcite, aragonite and vaterite CaCO3: Insights from first-principles calculations and implications for the I/Ca geochemical proxy. Geochim. Cosmochim. Acta 236, 351–360.
- Fu, W., Primeau, F., Moore, J.K., Lindsay, K., Randerson, J.T., 2018. Reversal of increasing tropical ocean hypoxia trends with sustained climate warming. Glob. Biogeochem. Cycles 32, 551–564.

- Galbraith, E.D., Jaccard, S.L., 2015. Deglacial weakening of the oceanic soft tissue pump: global constraints from sedimentary nitrogen isotopes and oxygenation proxies. Quat. Sci. Rev. 109, 38–48.
- Garcia, H.E., Weathers, K., Paver, C.R., Smolyar, I., Boyer, T.P., Locarnini, R.A., Zweng, M.M., Mishonov, A.V., Baranova, O.K., Seidov, D., Reagan, J.R., 2018. World Ocean Atlas 2018, volume 3: dissolved oxygen, apparent oxygen utilization, and oxygen saturation. NOAA Atlas NESDIS 83, 38.
- Glock, N., Eisenhauer, A., Milker, Y., Liebetrau, V., Schönfeld, J., Mallon, J., Sommer, S., Hensen, C., 2011. Environmental influences on the pore density of Bolivina spissa (Cushman). J. Foraminifer. Res. 41, 22–32.
- Glock, N., Schönfeld, J., Mallon, J., 2012. The functionality of pores in benthic foraminifera in view of bottom water oxygenation: a review. In: Altenbach, A.V., Bernhard, J.M., Seckbach, J. (Eds.), Anoxia: Evidence for Eukaryote Survival and Paleontological Strategies, Volume 21. Springer, pp. 539–552.
- Glock, N., Liebetrau, V., Eisenhauer, A., 2014. I/Ca ratios in benthic foraminifera from the Peruvian oxygen minimum zone: analytical methodology and evaluation as proxy for redox conditions. Biogeosciences (BG) 11, 7077–7095.
- Glock, N., Liebetrau, V., Eisenhauer, A., Rocholl, A., 2016. High resolution I/Ca ratios of benthic foraminifera from the Peruvian oxygen-minimum-zone: a SIMS derived assessment of a potential redox proxy. Chem. Geol. 447, 40–53.
- Glock, N., Erdem, Z., Wallmann, K., Somes, C.J., Liebetrau, V., Schönfeld, J., Gorb, S., Eisenhauer, A., 2018. Coupling of oceanic carbon and nitrogen facilitates spatially resolved quantitative reconstruction of nitrate inventories. Nat. Commun. 9 (1), 1–10.
- Glock, N., Liebetrau, V., Vogts, A., Eisenhauer, A., 2019. Organic heterogeneities in foraminiferal calcite traced through the distribution of N, S, and I measured with nanoSIMS: a new challenge for element-ratio-based paleoproxies? Front. Earth Sci. 7, 175.
- Gooday, A.J., 2003. Benthic foraminifera (Protista) as tools in deep-water palaeoceanography: Environmental influences on faunal characteristics. Adv. Mar. Biol. 46, 1–90.
- Gooday, A.J., Bett, B.J., Escobar, E., Ingole, B., Levin, L.A., Neira, C., Raman, A.V., Sellanes, J., 2010. Habitat heterogeneity and its influence on benthic biodiversity in oxygen minimum zones. Mar. Ecol. 31, 125–147.
- Gu, F., Zonneveld, K.A., Chiessi, C.M., Arz, H.W., Pätzold, J., Behling, H., 2017. Long-term vegetation, climate and ocean dynamics inferred from a 73,500 years old marine sediment core (GeoB2107-3) off southern Brazil. Quat. Sci. Rev. 172, 55–71.
- Hardisty, D.S., Lu, Z., Bekker, A., Diamond, C.W., Gill, B.C., Jiang, G., Lyons, T.W., 2017.
  Perspectives on Proterozoic surface ocean redox from iodine contents in ancient and recent carbonate. Earth Planet. Sci. Lett. 463, 159–170.
- Hardisty, D.S., Horner, T.J., Evans, N., Moriyasu, R., Babbin, A.R., Wankel, S.D., Moffet, J.W., Nielsen, S.G., 2021. Limited iodate reduction in shipboard seawater incubations from the Eastern Tropical North Pacific oxygen deficient zone. Earth Planet. Sci. Lett. 554, 116676.
- Hayward, B.W., Holzmann, M., Palwowski, J., Parker, J.H., Kaushik, T., Toyofukui, M.S., Tsuchiya, M., 2021. Molecular and morphological taxonomy of living *Ammonia* and related taxa (Foraminifera) and their biogeography. Micropaleontology 67, 1–84.
- Hendry, K.R., Robinson, L.F., Meredith, M.P., Mulitza, S., Chiessi, C.M., Arz, H., 2012. Abrupt changes in high-latitude nutrient supply to the Atlantic during the last glacial cycle. Geology 40 (2), 123–126.
- Hoogakker, B.A., Elderfield, H., Schmiedl, G., McCave, I.N., Rickaby, R.E., 2015. Glacial-interglacial changes in bottom-water oxygen content on the Portuguese margin. Nat. Geosci. 8, 40
- Hoogakker, B., Lu, Z., Umling, N., Jones, L., Zhou, X., Rickaby, R., Thunell, R., Cartapanis, O., Galbraith, E.D., 2018. Glacial expansion of oxygen-depleted seawater in the eastern tropical Pacific. Nature 562, 410–413.
- Huang, Z., Ito, K., Morita, I., Yokota, K., Fukushi, K., Timerbaev, A.R., Hirokawa, T., 2005. Sensitive monitoring of iodine species in sea water using capillary electrophoresis: vertical profiles of dissolved iodine in the Pacific Ocean. J. Environ. Monit. 7 (8), 804–808.
- Ito, K., Hirokawa, T., 2009. Iodine and iodine species in seawater: speciation, distribution, and dynamics. In: Preedy, V.R., Burrow, G.N., Watson, R.R. (Eds.), Comprehensive Handbook of Iodine–Nutritional, Biochemical, Pathological and Therapeutic Aspects. Academic Press Burlington, San Diego, London, pp. 83–92.
- Jacobel, A.W., Anderson, R., Jaccard, S.L., McManus, J., Pavia, F.J., Winckler, G., 2020. Deep Pacific storage of respired carbon during the last ice age: perspectives from bottom water oxygen reconstructions. Quat. Sci. Rev. https://doi.org/10.1016/j. quascirev.2019.106065. In Press.
- Jorissen, F., Fontanier, C., Thomas, E., 2007. Paleoceanographical proxies based on Deep-Sea Benthic foraminiferal assemblage characteristics. In: de Vernal, A. (Ed.), Proxies in Late Cenozoic Paleoceanography: Pt. 2: Biological tracers and biomarkers. Elsevier, pp. 263–326.
- Kaiho, K., 1994. Benthic foraminiferal dissolved-oxygen index and dissolved-oxygen levels in the modern ocean. Geology 22 (8), 719–722.
- Koho, K.A., Pina-Ochia, E., Geslin, E., Risgaard-Petersen, N., 2013. Vertical; migration, nitrogen uptake and denitrification: survival mechnisms of foraminifers (Globobulimina turgida) under low oxygen conditions. FEMS Microbiol. Ecol. 75, 272, 282
- Kowsmann, R.O., de Carvalho, M.D., 2002. Erosional event causing gas-venting on the upper continental slope, Campos Basin, Brazil. Cont. Shelf Res. 22, 2345–2354.
- Kuhnt, T., Friedrich, O., Schmiedl, G., Milker, Y., Mackensen, A., Lückge, A., 2013.
  Relationship between pore density in benthic foraminifera and bottom-water oxygen content. Deep-Sea Res. I Oceanogr. Res. Pap. 76, 85–95.
- Kuhnt, T., Schiebel, R., Schmiedl, G., Milker, Y., Mackensen, A., Friedrich, O., 2014. Automated and manual analyses of the pore density-to-oxygen relationship in Globobulimina turgida (Bailey). J. Foraminiferal Res. 44, 5–16.

- Licari, L., Mackensen, A., 2005. Benthic foraminifera off West Africa (1° N to 32° S): do live assemblages from the topmost sediment reliably record environmental variability? Mar. Micropaleontol. 55, 205–233.
- Lisiecki, L.E., Stern, J.V., 2016. Regional and global benthic  $\delta 180$  stacks for the last glacial cycle. Paleoceanography 31 (10), 1368–1394.
- Lu, Z., Jenkyns, H.C., Rickaby, R.E., 2010. Iodine to calcium ratios in marine carbonate as a paleo-redox proxy during oceanic anoxic events. Geology 38, 1107–1110.
- Lu, Z., Hoogakker, B.A., Hillenbrand, C.-D., Zhou, X., Thomas, E., Gutchess, K.M., Lu, W., Jones, L., Rickaby, R.E., 2016. Oxygen depletion recorded in upper waters of the glacial Southern Ocean. Nat. Commun. 7.
- Lu, W., Dickson, A.J., Thomas, E., Rickaby, R., Chapman, P., Lu, Z., 2019. Refining the planktic foraminiferal I/Ca proxy: results from the Southeast Atlantic Ocean. Geochimica et Cosmochimica Acta, In Press. https://doi.org/10.1016/j. gca.2019.1010.1025.
- Lu, W., Rickaby, R.E.M., Hoogakker, B.A.A., Rathburn, A.E., Burkett, A.M., Dickson, A.J., Martínez-Méndez, G., Hillenbrand, C., Zhou, X., Thomas, E., Lu, Z., 2020a. I/Ca in epifaunal benthic foraminifera: a semi-quantitative proxy for bottom water oxygen used in a multi-proxy compilation for glacial ocean deoxygenation. Earth Planet. Sci. Lett. 533, 116055.
- Lu, Z., Lu, W., Rickaby, R.E.M., Thomas, E., 2020b. Earth History of Oxygen and the iprOxy, Elements in Geochemical Tracers in Earth System Science. Cambridge University Press, Cambridge.
- Luther III, G.W., Campbell, T., 1991. Iodine speciation in the water column of the Black Sea. Dee. Sea Res. Part A. Oceanogr. Res. Pap. 38, S875–S882.
- Lutze, G., Thiel, H., 1989. Epibenthic foraminifera from elevated microhabitats; Cibicidoides wuellerstorfi and Planulina ariminensis. J. Foraminiferal Res. 19, 153–158.
- Mackensen, A., 2008. On the use of benthic foraminiferal d13C in palaeoceanography: constraints from primary proxy relationships. Geol. Soc. Lond. Spec. Publ. 303, 121–133.
- Mackensen, A., Hubberten, H.W., Bickert, T., Fischer, G., Fütterer, D., 1993. The  $\delta 13C$  in benthic foraminiferal tests of Fontbotia wuellerstorfi (Schwager) relative to the  $\delta 13C$  of dissolved inorganic carbon in southern ocean deep water: implications for glacial ocean circulation models. Paleoceanography 8, 587–610.
- McCorkle, D.C., Emerson, S.R., 1988. The relationship between pore water carbon isotopic composition and bottom water oxygen concentration. Geochim. Cosmochim. Acta 52, 1169–1178.
- Morford, J.L., Emerson, S., 1999. The geochemistry of redox sensitive trace metals in sediments. Geochim. Cosmochim. Acta 63 (11–12), 1735–1750.
- Pereira, L.S., Arz, H.W., Pätzold, J., Portilho-Ramos, R.C., 2018. Productivity evolution in the South Brazilian Bight during the last 40,000 years. Paleoceanogr. Paleoclimatol. 33, 1339–1356.
- Petersen, J., Riedel, B., Barras, C., Pays, O., Guihéneuf, A., Mabilleau, G., Schweizer, M., Meysman, F.J.R., Jorissen, F.J., 2016. Improved methodology for measuring pore patterns in the benthic foraminiferal genus Ammonia. Mar. Micropaleontol. 128, 1–13.
- Piña-Ochoa, E., Høgslund, S., Geslin, E., Cedhagen, T., Revsbech, N.P., Nielsen, L.P., Risgaard-Petersen, N., 2010a. Widespread occurrence of nitrate storage and denitrification among Foraminifera and Gromiida. Proc. Natl. Acad. Sci. 107 (3), 1148–1153.
- Piña-Ochoa, E., Koho, K.A., Geslin, E., Risgaard-Petersen, N., 2010b. Survival and life strategy of the foraminiferan Globobulimina turgida through nitrate storage and denitrification. Mar. Ecol. Prog. Ser. 417, 39–49.
- Podder, J., Lin, J., Sun, W., Botis, S., Tse, J., Chen, N., Hu, Y., Li, D., Seaman, J., Pan, Y., 2017. Iodate in calcite and vaterite: Insights from synchrotron X-ray absorption spectroscopy and first-principles calculations. Geochim. Cosmochim. Acta 198, 218–228.
- Portilho-Ramos, R.C., Cruz, A.P.S., Barbosa, C.F., Rathburn, A.E., Mulitza, S., Venancio, I.M., Schwenk, T., Rühlemann, C., Vidal, L., Chiessi, C.M., Silveira, C.S., 2018. Methane release from the southern Brazilian margin during the last glacial. Sci. Rep. 8, 1–9.
- Rathburn, A.E., Corliss, B.H., 1994. The ecology of living (stained) deep-sea benthic foraminifera from the Sulu Sea. Paleoceanography 9, 87–150.
- Rathburn, A.E., Willingham, J., Ziebis, W., Burkett, A.M., Corliss, B.H., 2018. A New biological proxy for deep-sea paleo-oxygen: Pores of epifaunal benthic foraminifera. Sci. Rep. 8, 9456.
- Reimer, P.J., Bard, E., Bayliss, A., Beck, J.W., Blackwell, P.G., Ramsey, C.B., et al., 2013. IntCal13 and Marine13 radiocarbon age calibration curves 0–50,000 years cal BP. Radiocarbon 55 (4), 1869–1887.
- Richirt, J., Champmartin, S., Schweizer, M., Mouret, A., Petersen, J., Ambari, A., Jorissen, F.J., 2019. Scaling laws explain foraminiferal pore patterns. Sci. Rep. 9, 1–11.
- Risgaard-Petersen, N., Langezaal, A.M., Ingvardsen, S., Schmid, M.C., Jetten, M.S., den Camp, H.J.O., van der Zwaan, G.J., 2006. Evidence for complete denitrification in a benthic foraminifer. Nature 443 (7107), 93–96.
- Rue, E.L., Smith, G.J., Cutter, G.A., Bruland, K.W., 1997. The response of trace element redox couples to suboxic conditions in the water column. Deep-Sea Res. I Oceanogr. Res. Pap. 44, 113–134.
- Schlitzer, R., 2020. Ocean Data View. https://odv.awi.de/.
- Schmidtko, S., Stramma, L., Visbeck, M., 2017. Decline in global oceanic oxygen content during the past five decades. Nature 542, 335–339.
- Schmittner, A., Somes, C.J., 2016. Complementary constraints from carbon (13C) and nitrogen (15N) isotopes on the glacial ocean's soft-tissue biological pump. Paleoceanography 31, 669–693.
- Schulz, H.D., Ayres Neto, A.A., Boetius, A., Enneking, K.F., Feseker, T., Funk, J., Gorke, M., Heidersdorf, F., Hensen, C., Heuer, V., Hill, H.G., Hinrichs, S., Kasten, S.,

- Klann, M., Lacerda de Souza, C.L., Martinez Briao, A., Meyer, S., Mulitza, S., Niebler, H.S., Ochsenhirt, W.T., Panteleit, B., Pfeifer, K., Schewe, F., Schwenk, T., Senorans, J.L., Siemer, S., Steinmetz, E., Wenzhofer, F., 2001. Part 2: Universität Hamburg
- Schweizer, M., 2006. Evolution and Molecular Phylogeny of Cibicides and Uvigerina (Rotaliida, Foraminifera) [PhD: University of Utrecht].
- Sen Gupta, B.K., Machain-Castillo, M.L., 1993. Benthic foraminifera in oxygen-poor habitats. Mar. Micropaleontol. 20, 183–201.
- Stramma, L., Johnson, G.C., Sprintall, J., Mohrholz, V., 2008. Expanding oxygenminimum zones in the tropical oceans. Science 320 (5876), 655–658.
- Tetard, M., Beaufort, L., Licari, L., 2017. A new optical method for automated pore analysis on benthic foraminifera. Mar. Micropaleontol. 136, 30–36.
- Tetard, M., Licari, L., Ovsepyan, E., Tachikawa, K., Beaufort, L., 2021. Toward a global calibration for quantifying past oxygenation in oxygen minimum zones using benthic Foraminifera. Biogeosciences 18 (9), 2827–2841.

- Tribovillard, N., Algeo, T.J., Lyons, T., Riboulleau, A., 2006. Trace metals as paleoredox and paleoproductivity proxies: an update. Chem. Geol. 232 (1–2), 12–32.
- Venturelli, R.E., Rathburn, A.E., Burkett, A.M., Ziebkis, W., 2018. Epifaunal foraminifera in an infaunal world: Insights into the inflkuence of heterogeneity on the benthic ecology of oxygen-poor, deep-sea habitats. Front. Mar. Sci. 5.
- Wirsig, C., Kowsmann, R.O., Miller, D.J., de Oliveira Godoy, J.M., Mangini, A., 2012. U/ Th-dating and post-depositional alteration of a cold seep carbonate chimney from the Campos Basin offshore Brazil. Mar. Geol. 329, 24–33.
- Wong, G.T., Brewer, P.G., 1977. The marine chemistry of iodine in anoxic basins. Geochim. Cosmochim. Acta 41 (1), 151–159.
- Yamamoto, A., Abe-Ouchi, A., Ohgaito, R., Ito, A., Oka, A., 2019. Glacial CO2 decrease and deep-water deoxygenation by iron fertilization from glaciogenic dust. Clim. Past 15, 981–996.
- Zhou, X., Thomas, E., Rickaby, R.E., Winguth, A.M., Lu, Z., 2014. I/Ca evidence for upper ocean deoxygenation during the PETM. Paleoceanography 29 (10), 964–975.